Geophysical Research Letters

Supporting Information for

Complex 3D Migration and Delayed Triggering of Hydraulic Fracturing-Induced Seismicity

Dawei Gao[1,2], Honn Kao[1,2]*, Bei Wang[1,2], Ryan Visser[2], Ryan Schultz[3], Rebecca Harrington[4]

[1]School of Earth and Ocean Sciences, University of Victoria, Victoria, British Columbia, Canada.

[2]Pacific Geoscience Centre, Geological Survey of Canada, Sydney, British Columbia, Canada.

[3]Department of Geophysics, Stanford University, Stanford, CA, USA.

[4]Ruhr University Bochum, Institute of Geology, Mineralogy, and Geophysics, Bochum, Germany.

Contents of this file

Introduction

This Supporting Information provides additional texts, figures, and tables to further support the arguments and findings presented in the main text. Texts S1 and S2 present the technical details of CC calculation and poroelastic modeling, respectively. Figure S1 displays the histogram of the 49 poorly correlated small earthquakes. Figure S2 shows the ΔP contribution in determining the ΔCFS with different permeabilities for the Mw 3.9 event. Table S1 summarizes the solid and fluid properties of each layer used in the poroelastic model. Table S2 presents the injection data.

Text S1. Technical Details of CC Calculation

When performing the waveform cross-correlation, the seismic waveforms are band-pass filtered from 1 to 10 Hz (*Schmittbuhl et al.,* 2016; *Warren-Smith et al*., 2017, 2018). The cross-correlation window is set to be 10 s, starting from 1 s before to 9 s after the theoretical predicted S-arrival (*Schultz et al*., 2017) based on the ak135 velocity model (*Kennett et al*., 1995). The choice of a 10-s window length is meant to capture the strongest and cleanest arrival and sufficient coda waves with a lower level of noise contamination. We do not choose a window starting from the P phase because the P waves are very small compared with the S phases, thus the result can be easily contaminated by noise (*Schultz et al*., 2017). The correlation is performed by sliding the waveform of one event from 4 s before the predicted S arrival of the other event to 4 s after, in one-sample increments. A ±4 s shift should be adequate to account for any predicted phase onset error due to an imperfect velocity model. The maximum value of the CC results during the sliding is defined as the final CC value of the event pair.

Text S2. Technical Details of Poroelastic Modeling

By assuming that the medium is homogeneous and isotropic, the evolution of pore pressure can be calculated by solving the coupled diffusion equations, as listed below (equivalent forms of the equations can be found in the literature, e.g., *Wang and Kumpel*, 2003),

$$\rho S \frac{\partial p}{\partial t} - \nabla \cdot \left(\rho \frac{\kappa}{\mu_d} \nabla p \right) = Q_m(x,t) - \rho \alpha \frac{\partial \varepsilon_{vol}}{\partial t} \tag{1}$$

$$S = \chi_f \theta + \chi_p (1 - \theta) \tag{2}$$

$$q = -\frac{\kappa}{\mu_d} \nabla p \tag{3}$$

where ρ is the pore fluid density, S is the linearized storage parameter, p is the fluid pore pressure, κ is the permeability of the medium, μ_d is its dynamic viscosity, Q_m is the volumetric flow rate for a fluid source, α is the Biot-Willis coefficient, ε_{vol} is the volumetric strain of the porous matrix, χ_f is the compressibility of the fluid, χ_p is the compressibility of the rock, θ is the porosity, and q is the velocity variable which gives a volume flow rate per unit area of porous material. The governing equations for the poroelastic model are then given by:

$$-\nabla \cdot \sigma = F_v \tag{4}$$

$$\sigma_{ij} = \frac{2G\nu}{(1-2\nu)} \varepsilon_{kk} \delta_{ij} + 2G \varepsilon_{ij} - \alpha p \delta_{ij} \tag{5}$$

$$\varepsilon_{ij} = \frac{1}{2} ((\nabla \boldsymbol{u})^T + \nabla \boldsymbol{u}) \tag{6}$$

where σ is the stress tensor, F_v is the volume force vector (i.e., $F_v = (\rho\theta + \rho_b)g$, where g is the acceleration of gravity, and ρ_b is the bulk density), δ_{ij} is the Kronecker delta (equal to 1 when $i = j$, and to 0 when $i \neq j$), G is Young's modulus, ν is the Poisson's ratio, and $\boldsymbol{u}$ is the displacement vector.

We build a 3D model of 5 km × 10 km × 5 km in the x, y and z directions, respectively, and split the model into four simplified layers (Table S1). From top to bottom, the four layers correspond to the upper sedimentary section, the Duvernay shale formation in which the HF horizontal wells are located, the lower sedimentary section, and the crystalline basement (*Bao and Eaton*, 2016). The solid and hydrogeological properties of each layer are listed in Table S1. Within the model, we set the so-called roller condition as the side solid boundaries, i.e., no vertical movement is permitted for the solid material on the boundary. We then set the bottom and top solid boundaries as fixed and free surfaces, respectively. Next, we set the fluid boundaries to have no flow. In addition, at the top, we add a standard atmospheric pressure, and set the pore pressure at the top surface to 0. Finally, we set the original fluid condition to be hydrostatic equilibrium.

In our model, besides the stimulation points, we assume that the HF operations have created a fracture zone surrounding the horizontal wells (note that the fracture zone is confined in the Duvernay shale layer), leading to an increased permeability compared to the unfractured shale formation. The width of the fractures centered at the stimulation points is set to be 200 m. We assume the permeability of the fractures to be 5×10^{-15} m^2, the same as that of the fluid channel but three orders higher than the low-permeability unfractured shale formation (1×10^{-18} m^2, Table S1). As mentioned in the main text, there are two inferred fault systems, i.e., the east sequence fault and the west sequence fault. In the model, we create two near-vertical faults on the basis of the Mw 3.9 and Mw 3.2 mainshock and their aftershock locations. We also assume that there is a near-horizontal basement fault connecting the two vertical fault systems (Figure 3). We set the permeability along the fault surface for the two vertical faults to be three orders of magnitude larger than the confining rock (Table S1), as the fault damage zone could enhance the permeability (*Yehya et al*., 2018). For the near-horizontal fault, it is worth noting that we have tested multiple permeability values, ranging from the same as the surrounding rock ($1 \times 10^{-18}\ m^2$) to five orders larger than the surrounding rock ($1 \times 10^{-13}\ m^2$, Figure 4b). This range of permeability includes not only the scenario of a high-permeable horizontal fault, but also one where the horizontal fault does not exist.

To simulate the multi-stage fluid injection process, we assume that fluid is injected at a single point of each stage, and the consecutive stages migrate along the horizontal well bore. Each stage's fluid injection rate is the ratio between stage injection volume and duration time (calculated from Table S2). The outcomes (stress tensor and pore pressure change) from the poroelastic modeling are then used to calculate the ΔCFS as discussed in the main text.

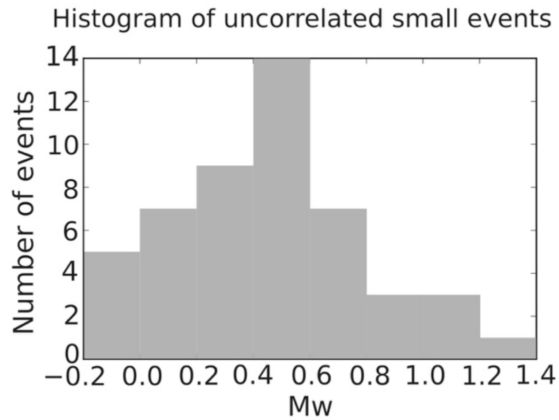

Figure S1. Histogram of the 49 poorly correlated small earthquakes.

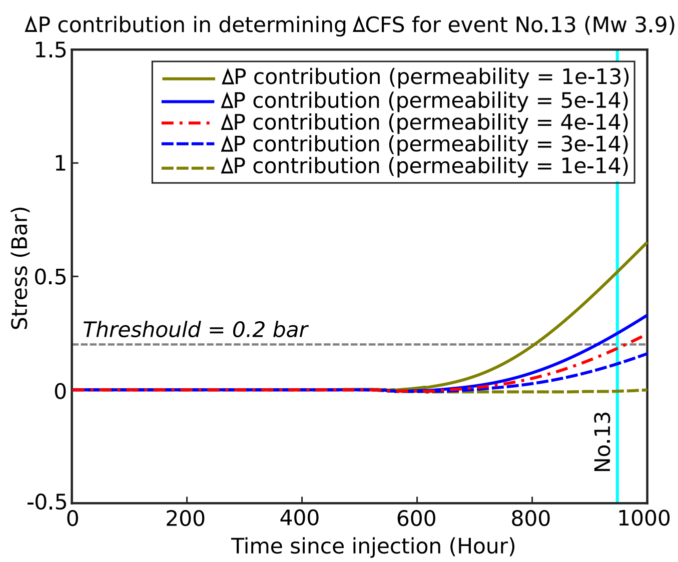

Figure S2. ΔP contribution in determining the ΔCFS for the Mw 3.9 event.

Table S1. Solid and fluid properties of each layer used in the model. Note that for the fracture zone, the permeability is 5×10^{-15} m^2 and the solid properties are the same as that of the confining Duvernay shale layer. For the two vertical faults, their solid properties are the same as the horizontal layers, and the permeability along the fault is 5×10^{-15} m^2.

	Layer 1	Layer 2 (HF layer)	Layer 3	Layer 4
Depth	0-3.3 km	3.3 km-3.4 km	3.4 km-4.1 km	4.1 km-5 km
Biot-Willis	0.7	0.7	0.7	0.7
P-wave velocity	5000 m/s	6100 m/s	6300 m/s	6900 m/s
S-wave velocity	2800 m/s	3520 m/s	3630 m/s	3983 m/s
Bulk Density (ρ_b)	2500 kg/m^3	2600 kg/m^3	2750 kg/m^3	2900 kg/m^3
Permeability	7.5×10^{-16} m^2	1×10^{-18} m^2	5×10^{-18} m^2	1×10^{-18} m^2
Porosity (θ)	0.1	0.05	0.05	0.08
Fluid density (ρ)	1000 kg/m^3	1000 kg/m^3	1000 kg/m^3	1000 kg/m^3
Fluid compressibility (χ_f)	4.5×10^{-10} Pa^{-1}	4.5×10^{-10} Pa^{-1}	4.5×10^{-10} Pa^{-1}	4.5×10^{-10} Pa^{-1}
Fluid dynamic viscosity (μ_d)	0.79×10^{-3} Pa*s	0.79×10^{-3} Pa*s	0.79×10^{-3} Pa*s	0.79×10^{-3} Pa*s

Table S2. Injection data.

Well	Stage	Stage-start	Stage-end	Total Fluid (m^3)
1	1	17-12-2014--00:38	17-12-2014--04:02	1417
1	2	17-12-2014--18:08	17-12-2014--21:30	1288
1	3	18-12-2014--04:17	18-12-2014--07:10	1196
1	4	18-12-2014--13:53	18-12-2014--16:31	1196
1	5	18-12-2014--21:37	19-12-2014--00:11	1220
1	6	19-12-2014--04:50	19-12-2014--07:25	1217
1	7	19-12-2014--14:30	19-12-2014--18:47	1367
1	8	19-12-2014--23:44	20-12-2014--02:16	1123
1	9	20-12-2014--08:46	20-12-2014--11:01	1065
1	10	21-12-2014--00:33	21-12-2014--02:50	1101
1	11	21-12-2014--10:23	21-12-2014--13:36	1189
1	12	30-12-2014--03:43	30-12-2014--06:00	907.4
1	13	31-12-2014--11:45	31-12-2014--14:23	1199
1	14	31-12-2014--23:28	01-01-2015--02:26	1234
1	15	01-01-2015--11:35	01-01-2015--14:20	1266
1	16	01-01-2015--22:40	02-01-2015--01:34	1226
1	17	03-01-2015--22:43	04-01-2015--01:45	1333
1	18	04-01-2015--11:17	04-01-2015--13:56	1265
1	19	04-01-2015--21:24	05-01-2015--00:21	1268
1	20	05-01-2015--07:21	05-01-2015--10:26	1210.7
1	21	05-01-2015--18:17	05-01-2015--21:10	1174
1	22	06-01-2015--04:29	06-01-2015--06:55	1102
1	23	06-01-2015--17:30	06-01-2015--20:33	1301
1	24	07-01-2015--08:54	07-01-2015--11:05	987
1	25	09-01-2015--14:35	09-01-2015--17:26	1084
2	1	17-12-2014--06:52	17-12-2014--10:44	1253
2	2	20-12-2014--03:56	20-12-2014--07:00	1128
2	3	20-12-2014--13:06	20-12-2014--15:55	1219
2	4	21-12-2014--04:44	21-12-2014--07:21	1282
2	5	29-12-2014--17:52	30-12-2014--01:40	1294

2	6	30-12-2014--11:45	30-12-2014--14:36	1290
2	7	30-12-2014--20:26	30-12-2014--23:11	1305
2	8	31-12-2014--04:33	31-12-2014--07:20	1309
2	9	31-12-2014--17:58	31-12-2014--20:53	1192
2	10	01-01-2015--06:03	01-01-2015--08:49	1324
2	11	01-01-2015--16:46	01-01-2015--19:02	1087
2	12	02-01-2015--03:29	02-01-2015--06:18	1219
2	13	02-01-2015--10:36	02-01-2015--13:19	1278
2	14	03-01-2015--00:58	03-01-2015--20:28	1834
2	15	04-01-2015--06:01	04-01-2015--08:39	1267
2	16	04-01-2015--16:04	04-01-2015--18:42	1266
2	17	05-01-2015--02:36	05-01-2015--05:20	1218
2	18	05-01-2015--12:44	05-01-2015--15:17	1171
2	19	05-01-2015--23:03	06-01-2015--01:45	1212
2	20	06-01-2015--13:02	06-01-2015--15:22	1056
2	21	06-01-2015--21:58	07-01-2015--00:35	1101
2	22	07-01-2015--04:03	07-01-2015--06:49	1267
2	23	07-01-2015--21:09	07-01-2015--23:45	957
2	24	08-01-2015--03:35	08-01-2015--06:26	1144
2	25	08-01-2015--10:42	08-01-2015--13:04	1010

124